



Impedance Tube Solution for Helmholtz Resonator Prototyping

David Jun¹ · Josef Plasek¹

Received: 15 May 2024 / Accepted: 24 November 2024 / Published online: 21 January 2025
© The Author(s) 2024

Abstract

Transfer function method impedance tube measurement is a well-known approach used for determining acoustical properties of mostly porous materials. This paper presents a prototype of impedance tube together with the software solution published under open-source license. The prototype is developed specifically for experimental design of Helmholtz resonators. For room acoustic purposes, these are difficult to sufficiently characterize by other methods because of their highly frequency dependent complex-valued pressure reflection factor resulting in large phase shifts happening upon reflection. The main benefits of the presented method are the movable rigid termination operated by a stepper motor and the use of open-source libraries as well as widely available hardware for the whole measurement.

Keywords Impedance tube · Transfer function · Helmholtz resonator · Harmonic distortion · Signal filtering

1 Introduction

In room acoustics, we usually encounter three types of absorption measurements: reverberation room, free field and impedance tube measurements. The latter, also commonly known as Kundt tube method is widely spread because of small sample size, well-defined normal incidence boundary conditions and speed. This allows for numerical simulation validation [1–7] as well as for prototyping and optimization.

The original Kundt tube was invented by August Kundt in 1866 [8]. The older method directly measuring the standing wave ratio (SWR) is being replaced with the transfer function-based methods working with fixed microphone positions. Two main variants were established—single-microphone method [9–11] and two-microphone method [12–15]. An overview of these and other acoustic impedance measurement methods is given by Hiremath et al. [16]. All three above mentioned methods are described in various standards, ISO 10534–1 [17] and ISO 10534–2 [18] in the European context.

There are several reasons why the standing wave method is nowadays used mostly for the verification of results obtained by other methods. The main ones are probably the longer measurement duration and the rougher frequency resolution

of the measurement. Thanks to some theory and digital signal processing, transfer function method overcomes these drawbacks and is more versatile in its usability.

The main problem of the standardized two-microphone method is the relatively narrow frequency bandwidth of the measurements. The partial solution to this problem was presented by Schneider et al. [19] who added multiple microphones to one cross sectional plane of the tube. In general, multiple tube diameters are still needed to measure extended range of frequencies [20].

Slightly different branch of research connected to this topic was focusing on measurement signals suitable for acoustic measurements. From today's perspective, the deterministic signals seem to work the best. Maximum length sequences (MLS) [21] and swept sines [22] are probably the most used examples.

This paper presents a prototype impedance tube built to measure Helmholtz resonators in the region of approximately 63–500 Hz. Attention is paid mainly to two innovative aspects of this prototype. First, hardware and software solution of the tube is described as well as the movable rear wall controlled by a stepper motor. Second, the capabilities of this device are discussed and a solution for harmonic distortion filtering is described.

✉ David Jun
David.Jun@vut.cz

¹ Faculty of Civil Engineering, Brno University of Technology, Brno, Czech Republic

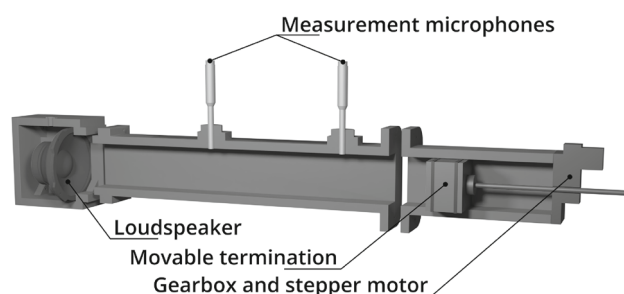


Fig. 1 A scheme of the presented impedance tube prototype

2 Methods

2.1 Hardware Solution

Figure 1 shows the schematic 3D section view on the tube. It is divided into three main parts: Source part, microphone part and specimen part. The microphone and specimen parts have a square inner cross section of 100×100 mm, the source part is almost cubic with the cross section of 172×172 mm. The cavity depth in the specimen part is variable from 0 up to 200 mm, the spacing of the microphone part is 101.5–298.5–300 mm (specimen to microphone—distance of the microphones—approximate microphone to source distance). All the three parts are made from 18mm thick birch plywood. The connections within one part are mostly glued. Parts are connected by M5 bolts and special nuts driven into the plywood. Screwed connections are sealed with 1mm thick EPDM stripes (except for the one used for placing a specimen). FDM 3D printing has been used to make custom shaped parts out of PLA and PETG plastics. Laser cutting has been used for making EPDM sealings (1mm and 6mm thick) and specimens (both PES fiber boards and plywood). The specimen can be placed in the tube in two ways: Either fitted in the specimen part or placed in between the flanges connecting the microphone part and source part. The latter way is used for measuring Helmholtz resonator formed by perforated board and cavity. It is the measurement of perforated plate-based Helmholtz resonators, which motivated some geometrical choices, which would be otherwise considered not advantageous. First, the square cross section is beneficial when considering larger-scale final products of repeating perforation patterns. Second, the larger lateral dimensions allow for a larger variability of neck geometry and spacing. This becomes important when tuning resonators towards lower frequencies or lower absorption.

Source part contains a PES fiber board infill, a loudspeaker and a Speakon connector. The speaker is a low to medium frequency range 6.5" loudspeaker with the working frequency range of 40 to 4500 Hz, resonance frequency 56.2 Hz, nominal impedance 8Ω , and nominal power handling up

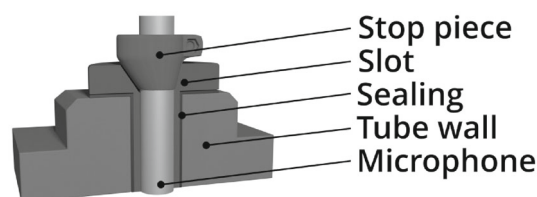


Fig. 2 Microphone slot scheme consisting of 3D printed asymmetrical stop piece and slot, EPDM sealing, plywood wall of the tube and microphone

to 60 W RMS. The loudspeaker is elastically mounted over 3D printed PETG flange and laser-cut 6mm thick EPDM spacer.

Microphone part contains slots for microphone insertion. The slot is shown in Fig. 2. 3D printed PLA insertions are put inside the drilled hole and separated from the tube with 1 mm EPDM sealing to avoid transmission of tube vibrations to the microphone. Microphone rotation around the vertical axis is constrained by the asymmetrical stop piece.

Specimen part is formed by the tube itself, the termination block with the attached threaded rod, gearbox and the stepper motor. The termination block is glued from 4 layers of 18 mm plywood. The airtightness is secured by two slightly compressed rings of 6mm EPDM, laser cut to fit two slots milled around the block. On one side, the M10 threaded rod is attached to the block, without the possibility of rotation. The rod then goes through the gearbox containing M10 nut attached to one of the gears 0.4 Nm NEMA 17 style motor is used for the termination movements.

Electronics of the measuring set are stored in a 3U 19" rack. The rack contains Raspberry Pi SBC, audio interface Focusrite Scarlett 18i20 3rd Gen, Power amplifier t.amp S-75 MKII and additional storage space for the microphones Behringer ECM8000, the stepper driver DRV8825 and the temperature and humidity sensor HTU21D.

3 Software Solution

The measurement is handled by a custom open-source Python library [23] called *imptube* [24] and Jupyter notebook scripts [25]. The problem can be split into three parts: individual sub-measurements, audio processing and moving the rigid termination. The custom module contains three main objects: *Measurement*, *Tube* and *Sample*.

Measurement object contains information about the measurement from the perspective of signal, routing and frequency bandwidth.

Tube object contains information about the tube geometry.

Sample object represents the sample and measurement boundary conditions.

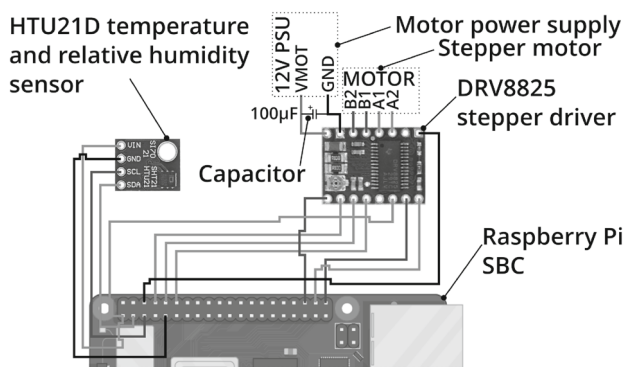


Fig. 3 HTU21D sensor and DRV8825 driver connection scheme

3.1 Sub-measurement

Function called *measure* is used for measurements as well as for calibration. It was implemented with use of *sounddevice* [26] module enabling for simultaneous playback and recording. The *SciPy* [27] library is used for logarithmic sweep generation and pre-processing.

3.2 Audio processing

Uses also the *SciPy* library. Initially, the time-domain measured signal from both microphones is converted using Fast Fourier transform (FFT). The whole processing is then done in the frequency domain. The main output is a transfer function calculated as a ratio between the data captured on both microphones:

$$H_{12}(f) = \frac{p_2(f)}{p_1(f)} \tag{1}$$

where $H_{12}(f)$ is a transfer function between position 1 and 2 on the tube and $p_1(f)$, $p_2(f)[-]$ are spectra of the signals measured with microphone 1 and 2 (counted from the loudspeaker end). The results are corrected by a calibration factor measured in advance of specimen measurement. It aims on compensation of the amplitude and phase mismatch between the microphones [18].

3.3 Movable rigid termination

Utilizes the GPIO header of the Raspberry Pi SBC and the DRV8825 stepper driver. A connection scheme is shown in Fig. 3. A custom module was written to operate the stepper motor using *RPi.GPIO* [28] and *NumPy* [29] libraries.

4 Results and Discussion

As described in previous sections, a prototype impedance tube was made. A photograph is shown in Fig. 4. The bandwidth of the measurement is rather limited and is caused by the spacing of the two microphones. The ISO standard recommends the spacing to not be lower than 5% of the lowest wavelength of interest, which in this case sets the limit to approximately 57 Hz, assuming the speed of sound $c_0 = 343m/s$. The higher limit then equals to $f_u = 0,45c_0/s = 515Hz$. To stay on the safe side, the approximate range is narrowed down to 63–500 Hz. Note that the bandwidth could be further extended by adding a third microphone between the original two to get to the limit motivated by avoiding lateral resonances given by $f_u = 0,5c_0/d = 1715Hz$, where $d[m]$ is the largest cross sectional side of the tube.

This section is going to describe the typical normal incidence absorption coefficient $\alpha_n[-]$ result when measuring mainly Helmholtz resonators (HR). A special attention is paid to the deviations occurring in the measured courses.

A typical output of the measurement can be seen in Fig. 5. The figure shows HR measurements of cavity depth varying between 60 and 180 mm, spaced by 40 mm each. The most evident and not expected feature of the resulting courses is the amount of oscillations. The deviations are harmonic and vary in amplitude over the measured spectrum. To visually demonstrate the harmonic nature of the deviations, the measurement sweep length was chosen shorter than in other presented measurements.

5 Deviation Source From Signal Perspective

As visible on Fig. 5, the deviations are harmonic.

Figure 6 shows the spectrogram of a measurement recording. The side sweeps above the fundamental tone represents the harmonic distortion occurring in the tube. The time difference between the first upper harmonic tone and the fundamental tone $t^*[s]$ stays constant across the measurement and is equal to the sweep rate of the measurement sweep, which expresses the time span of one octave evolution. It also appears in the impulse response (IR) as the time span between the main impulse and the first backward shifted impulse expressing the first upper harmonic. It can be related to the frequency span of one deviation revolution $\Delta f[Hz]$ visible in Fig. 5 by

$$t^* = \frac{1}{\Delta f} \tag{2}$$

The same equation is valid also for the other upper harmonics. As pointed out by Müller and Massarani [30], using

Fig. 4 A photo of the impedance tube prototype

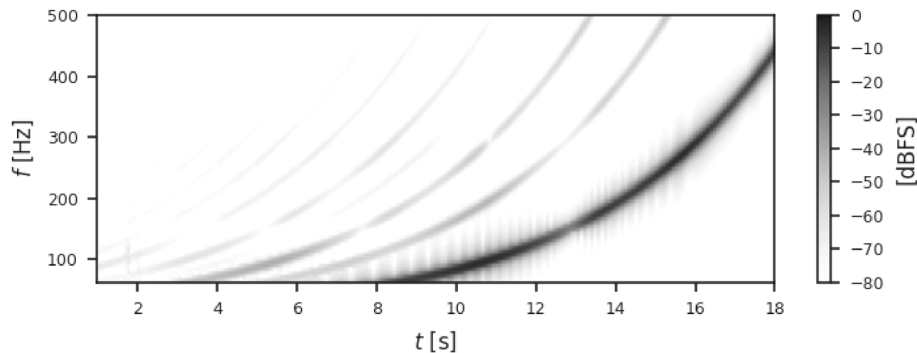
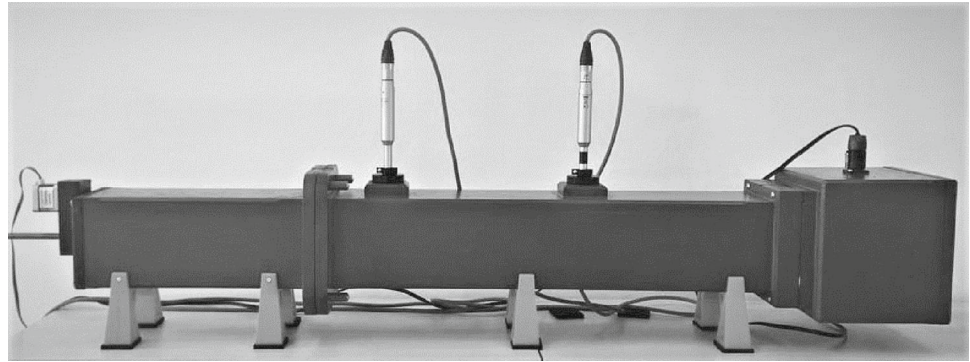


Fig. 5 Logarithmic sweep measurement spectrogram for a resonator. Resonator geometry is the same as in Fig. 6 only the cavity depth is 200 mm. The main (loudest, darkest) sweep is accompanied by its upper harmonics showing the harmonic distortion of the measurement. Sweep parameters: sampling rate $f_s = 48$ kHz, number of samples $N = 1,048,576$, duration $T = 21,8$ s, frequency range of 10 to 1000 Hz, sweep rate 0,30 oct./s, no averaging, peak normalized

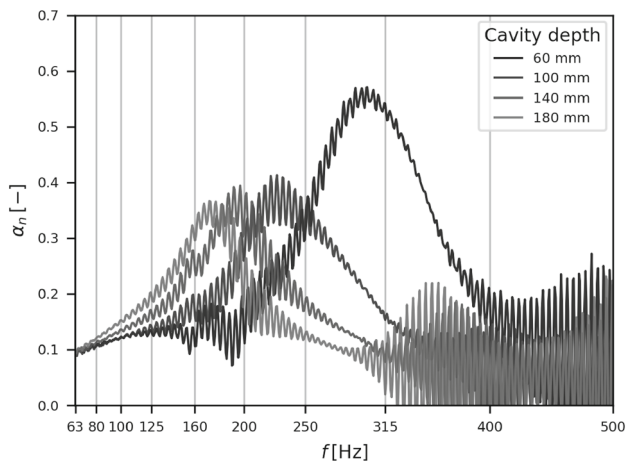


Fig. 6 Unfiltered Helmholtz resonator absorption measurement. Perforated medium density fiberboard (MDF) with neck radius $r = 12,5$ mm, neck spacing $D = 100$ mm, plate thickness $t = 9$ mm. The cavity depth varies. Sweep parameters: sampling rate $f_s = 48$ kHz, number of samples $N = 65,536$, duration $T = 1,37$ s, frequency range of 10 to 1000 Hz, sweep rate of 4,87 oct./s, no averaging

random excitation signals like MLS or white noise does not come with this behavior and harmonic distortion is spread across the whole IR duration in the form of a raised noise

floor. This can be lowered by longer averaging times, but not avoided. In the case of sweeps, harmonic distortion can be precisely measured or completely filtered from the measurement, as follows.

6 Deviation Filtration

A filtering solution was developed to filter harmonic distortion out of the measured audio. For that purpose, procedures described in [30] were adapted.

6.1 Preprocessing

First, the original measured time sequences $p_n(s)$ (n for microphone number) as well as the reference (source input) sweep $p_{\text{ref}}(s)$ are extended with zeros of the same length N as the original signal. This is done to get longer time span between the fundamental impulse response and the backwards shifted harmonic distortion peaks. After that, source sweep is shifted to the left by samples corresponding to the half-octave span in the logarithmic sweep. This keeps the whole main pulse of the later calculated IR at the beginning of the time sequence and makes windowing slightly more

intelligible. To filter out all the harmonic distortion, it is beneficial to work with longer sweeps with slower sweep rates. This leads to a good separation between the main impulse and the first upper harmonic related one, avoiding accidental overflowing of the distortion related impulse to the beginning of the IR.

6.2 Filtering

Time sequences $p_n(s)$ and $p_{ref, shifted}(s)$ are then transformed to the frequency domain using FFT. The transfer function $H_{ref, n}(f)$ between the reference spectrum $p_{ref, shifted}(f)$ and the measured spectrum $p_n(f)$ is obtained as

$$H_{ref, n}(f) = \frac{p_n(f)}{p_{ref, shifted}(f)}, \tag{3}$$

This transfer function is then filtered using a filter composed of Hann half windows positioned at the lowest and highest one-third octave of the reference sweep bandwidth, ones for the frequency bins in between the half windows and zeros outside of the bandwidth. The sweep frequency range needs to be, respectively, larger than the impedance tube working frequency range to keep the relevant part of the signal and the frequencies outside of it gradually diminish to zero.

In the next step, the inverse Fourier transform is applied to the transfer function. The second half of the resulting impulse response $H_{ref, n}(s)$ contains the harmonic distortion side-peaks; and therefore, it is replaced by zeros. This filtered impulse response $H_{ref, n, filtered}(s)$ is then transformed again using FFT and the resulting transfer function $H_{ref, n, filtered}(f)$ multiplied with the reference sweep:

$$p_{n, filtered}(f) = H_{ref, n, filtered}(f) \cdot p_{ref, shifted}(f) \tag{4}$$

after this procedure, a spectrum representing the measured sweep without harmonic distortion $p_{n, filtered}(f)$ is obtained and can be used for further calculations. The comparison between absorption coefficient calculated without and with the filtration is shown in Fig. 7.

7 Solution Verification on A Porous Sample Measurement

For further assessment of the solution, porous sample measurement results are compared between different setups. Porous sample consisted of three layers of 5 cm thick PES fiber board with flow resistivity $\sigma = 4.01 \text{ kPa} \cdot \text{s} \cdot \text{m}^{-2}$. Figure 8 shows the compared measurements. The first one is performed in the impedance tube prototype with use of the *imptube* software solution, the second in the impedance

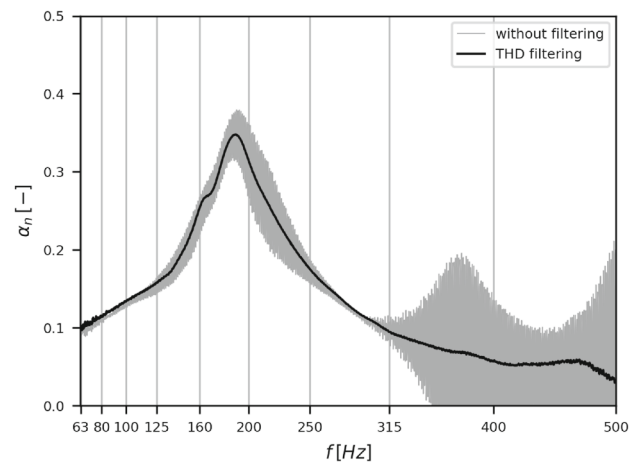


Fig. 7 Total harmonic distortion (THD) filtration effect example compared to measurement without filtering. The sample is the same as in Fig. 5, cavity depth is 140 mm. Sweep parameters: sampling rate $f_s = 48$ kHz, number of samples $N = 262,144$, duration $T = 5,46$ s, frequency range of 10 to 1000 Hz, sweep rate 1,22 oct./s, no averaging

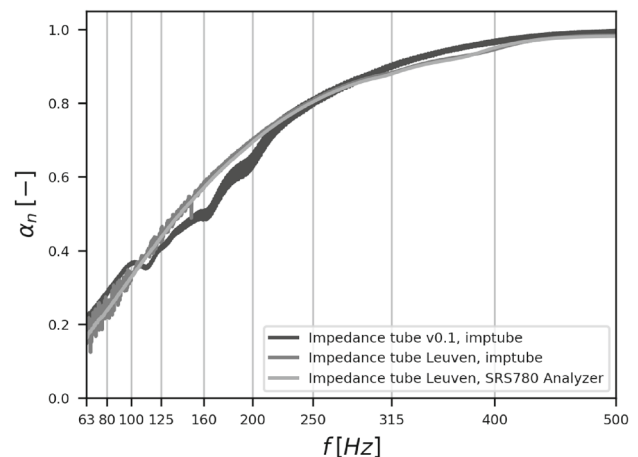


Fig. 8 A comparison between absorption measurements taken in different setup alterations. The sample consists of 3 layers of 5 cm thick polyester fiber board ($\sigma = 4,01 \text{ kPa} \cdot \text{s} \cdot \text{m}^{-2}$). No distortion filtering is applied. Sweep parameters: sampling rate $f_s = 48$ kHz, number of samples $N = 262,144$, duration $T = 5,46$ s, frequency range of 10 to 1000 Hz, sweep rate 0,30 oct./s, averaged over 4 sweep runs

tube from the acoustic laboratory at KU Leuven with use of the same software and sound card, but using Brüel&Kjær microphone preamplifiers and microphones. The third one is then measured with the complete laboratory setup containing SRS780 Analyzer. The only bigger difference in the courses can be found around 160Hz third octave band. This dip was seen in all measurements performed for the comparison and it was changing based on specimen placement. It is also probably partially related to limited rigidity of the termination wall, since some of its influence systematically appears also in other measurements performed.

8 Conclusions

An impedance tube prototype for measuring Helmholtz resonators has been developed. The prototype consists of novel hardware and software solution with the following main features: (a) Termination wall is operated by a stepper motor, (b) the software solution is published under open-source license as Python library called *imptube* [24], (c) consumer grade hardware is used for the measurements and (d) the harmonic distortion is filtered out completely from the captured signals, removing the cause of unwanted harmonic deviations in the output data. This filtration is also possibly compensating for lower quality hardware, while avoiding data corruption. The prototype was compared to another laboratory setup, which has shown that the differences in results are minor and mainly caused by the hardware solution of the tube and the quality of the microphones and loudspeaker used. In this context, the rigid termination quality and the overall rigidity are confirmed to be a key component of the impedance tube method. Future iterations of the setup should consider termination wall material, which would provide a higher impedance mismatch, such as steel. The software and acquisition parts are almost interchangeable. Even though the existing setup in the acoustic laboratory at KU Leuven performs without any doubts, there are at least two possible reasons for using *imptube*-based solution instead:

1. It is possible to easily make a parametrized measurement routine, which is generally less prone to errors than manually adjusted measurements. (e.g., different levels of loudspeaker excitation, cavity depths, source signals, or other depending on the specific experiment design)
2. No need for other hardware than either relatively cheap or already available in most acoustics-oriented facilities, schools.

When using high quality hardware, the harmonic distortion related to the sample under test can be of interest. The presented solution also enables without many constraints for an experimental approach where specific impedance tube is built for a sample geometry constrained by other factors, such as production or modularity.

Acknowledgements This research was possible thanks to the specific university research project at the Brno University of Technology, FAST-J-23-8284 (2023). Special thanks go to prof. Christ Glorieux for his help with the theory and troubleshooting.

Funding Open access publishing supported by the institutions participating in the CzechELib Transformative Agreement. Fakulta Stavební, Vysoké Učení Technické v Brně, FAST-J-23-8284, David Jun

Open Access This article is licensed under a Creative Commons Attribution 4.0 International License, which permits use, sharing, adaptation, distribution and reproduction in any medium or format, as long as you

give appropriate credit to the original author(s) and the source, provide a link to the Creative Commons licence, and indicate if changes were made. The images or other third party material in this article are included in the article's Creative Commons licence, unless indicated otherwise in a credit line to the material. If material is not included in the article's Creative Commons licence and your intended use is not permitted by statutory regulation or exceeds the permitted use, you will need to obtain permission directly from the copyright holder. To view a copy of this licence, visit <http://creativecommons.org/licenses/by/4.0/>.

References

1. TAM, C. K. W., KURBATSKII, K. A., AHUJA, K. K. and GAETA, R. J. A Numerical and Experimental Investigation of The Dissipation Mechanisms of Resonant Acoustic Liners. *Journal of Sound and Vibration*. Online. 16 August 2001. 245, 3, 545–557. [Accessed 21 January 2023]. <https://doi.org/10.1006/jsvi.2001.3571>.
2. TAM, C. K. W., JU, H., JONES, M. G., WATSON, W. R. and PARROTT, T. L. A computational and experimental study of slit resonators. *Journal of Sound and Vibration*. Online. 21 June 2005. 284, 3, 947–984. [Accessed 21 January 2023]. <https://doi.org/10.1016/j.jsv.2004.07.013>.
3. TAM, Christopher K. W., JU, H., JONES, M. G., WATSON, W. R. and PARROTT, T. L. A computational and experimental study of resonators in three dimensions. *Journal of Sound and Vibration*. Online. 22 November 2010. 329, 24, 5164–5193. [Accessed 21 January 2023]. <https://doi.org/10.1016/j.jsv.2010.06.005>.
4. LACOMBE, R., FÖLLER, S., JASOR, G., POLIFKE, W., AURÉGAN, Y. and MOUSSOU, P. Identification of aero-acoustic scattering matrices from large eddy simulation: Application to whistling orifices in duct. *Journal of Sound and Vibration*. Online. 30 September 2013. 332, 20, 5059–5067. [Accessed 21 January 2023]. <https://doi.org/10.1016/j.jsv.2013.04.036>.
5. PASQUAL, Alexander Mattioli and LARA, Luana Torquete. Time-domain simulation of acoustic impedance tubes. *Journal of the Brazilian Society of Mechanical Sciences and Engineering*. Online. 1 January 2017. 39, 1, 67–79. [Accessed 21 January 2023]. <https://doi.org/10.1007/s40430-016-0515-9>.
6. KHRAMTSOV, I. V., KUSTOV, O. Yu., FEDOTOV, E. S. and SINER, A. A. On Numerical Simulation of Sound Damping Mechanisms in the Cell of a Sound-Absorbing Structure. *Acoustical Physics*. Online. 1 July 2018. 64, 4, 511–517. [Accessed 21 January 2023]. <https://doi.org/10.1134/S1063771018040073>.
7. HASHEMI, Z., MONAZZAM, M. R. and FAHIM, A. Estimation of Sound Absorption Performance of Complex Perforated Panel Absorbers by Numerical Finite Element Method and Examining the Role of Different Layouts Behind It. *Fluctuation and Noise Letters*. Online. 16 July 2019. [Accessed 21 January 2023]. <https://doi.org/10.1142/S0219477519500135>.
8. KUNDT, August. Ueber eine neue Art akustischer Staubfiguren und über die Anwendung derselben zur Bestimmung der Schallgeschwindigkeit in festen Körpern und Gasen. *Annalen der Physik und Chemie*. Online. 1866. 203, 4, 497–523. [Accessed 13 September 2022]. <https://doi.org/10.1002/andp.18662030402>.
9. FAHY, F. J. Rapid method for the measurement of sample acoustic impedance in a standing wave tube. *Journal of Sound and Vibration*. Online. 8 November 1984. 97, 1, 168–170. [Accessed 21 January 2023]. [https://doi.org/10.1016/0022-460X\(84\)90478-4](https://doi.org/10.1016/0022-460X(84)90478-4).
10. CHU, W. T. Single-microphone method for certain applications of the sound intensity technique. *The Journal of the Acoustical Society of America*. Online. November 1985. Vol. 78, no. S1, p. S60–S60. [Accessed 21 January 2023]. <https://doi.org/10.1121/1.2022905>.

11. CHU, W. T. Transfer function technique for impedance and absorption measurements in an impedance tube using a single microphone. *The Journal of the Acoustical Society of America*. Online. August 1986. 80, 2, 555–560. [Accessed 21 January 2023]. <https://doi.org/10.1121/1.394050>.
12. Seybert, A.F., Ross, D.F.: Experimental determination of acoustic properties using a two-microphone random-excitation technique. *J. Acoust. Soc. Am.* **61**(5), 1362–1370 (1977). <https://doi.org/10.1121/1.381403>
13. CHUNG, J. Y. and BLASER, D. A. Transfer function method of measuring in-duct acoustic properties. I. Theory. *Journal of the Acoustical Society of America*. 1980. 68, 3, 907–913. <https://doi.org/10.1121/1.384778>.
14. CHUNG, J. Y. and BLASER, A. Transfer function method of measuring in-duct acoustic properties. II. Experiment. *Journal of the Acoustical Society of America*. 198068, 3, 914–921. <https://doi.org/10.1121/1.384779>.
15. FUJIKAWA, Takeshi and SEYBERT, A. F. Transfer function method for measuring characteristic impedance and propagation constant of porous materials. *Journal of the Acoustical Society of America*. 1989. 86, 2, 637–643. <https://doi.org/10.1121/1.398241>.
16. HIREMATH, Nandeesh, KUMAR, Vaibhav, MOTAHARI, Nicholas and SHUKLA, Dhwanil. An Overview of Acoustic Impedance Measurement Techniques and Future Prospects. *Metrology*. Online. September 2021. 1, 1, 17–38. [Accessed 11 January 2023]. <https://doi.org/10.3390/metrology1010002>.
17. *ISO 10534-1:1996, Acoustics – determination of sound absorption coefficient and impedance in impedance tubes. Part 1: Method using standing wave ratio*. 1996. Geneva, Switzerland : International Organization for Standardization.
18. *ISO 10534-2:1998, Acoustics-Determination of sound absorption coefficient and impedance in impedance tubes-Part 2: Transfer-function method*. 1998. Geneva, Switzerland : International Organization for Standardization.
19. SCHNEIDER, W., LEISTNER, Michael, ZICKMANTEL, Frank and TIPPKEMPER, R. Large scale impedance tubes. *Proc. CFA/DAGA'04*, Strasbourg, 1 January 2004. 469–470.
20. COX, Trevor J. and D'ANTONIO, Peter. *Acoustic absorbers and diffusers: Theory, design and application*. 3rd ed. Taylor, 2017. ISBN 978-0-415-47174-9.
21. RIFE, Douglas D. and VANDERKOOY, John. Transfer-Function Measurement with Maximum-Length Sequences. *Journal of the Audio Engineering Society*. Online. 1 June 1989. 37, 6, 419–444. [Accessed 13 September 2022]. Available from: <https://www.aes.org/e-lib/browse.cfm?elib=6086>
22. FARINA, Angelo. Simultaneous Measurement of Impulse Response and Distortion With a Swept-Sine Technique. In : *Audio Engineering Society Convention 108*. Online. Paris, 2000. Available from:
23. VAN ROSSUM, G. and DRAKE, F. L. *Python 3 reference manual*. . Scotts Valley, CA : CreateSpace, 2009. ISBN 1-4414-1269-7.
24. JUN, David. *imptube*. Online. 0.0.2. Python 3. [Accessed 12 December 2023]. Available from:
25. KLUYVER, Thomas, RAGAN-KELLEY, Benjamin, PÉREZ, Fernando, GRANGER, Brian, BUSSONNIER, Matthias, FREDERIC, Jonathan, KELLEY, Kyle, HAMRICK, Jessica, GROUT, Jason, CORLAY, Sylvain, IVANOV, Paul, AVILA, Damián, ABDALLA, Safia and WILLING, Carol. Jupyter Notebooks – a publishing format for reproducible computational workflows. In : LOIZIDES, F. and SCHMIDT, B. (eds.), *Positioning and power in academic publishing: Players, agents and agendas*. 2016. p. 87–90. *python-sounddevice*. Online. 0.4.5. Python 3. [Accessed 15 September 2022]. Available from:
27. VIRTANEN, Pauli, GOMMERS, Ralf, OLIPHANT, Travis E., HABERLAND, Matt, REDDY, Tyler, COURNAPEAU, David, BUROVSKI, Evgeni, PETERSON, Pearu, WECKESSER, Warren, BRIGHT, Jonathan, VAN DER WALT, Stéfan J., BRETT, Matthew, WILSON, Joshua, MILLMAN, K. Jarrod, MAYOROV, Nikolay, NELSON, Andrew R.J., JONES, Eric, KERN, Robert, LARSON, Eric, CAREY, C. J., POLAT, İlhan, FENG, Yu, MOORE, Eric W., VANDERPLAS, Jake, LAXALDE, Denis, PERKTOLD, Josef, CIMRMAN, Robert, HENRIKSEN, Ian, QUINTERO, E. A., HARRIS, Charles R., ARCHIBALD, Anne M., RIBEIRO, Antônio H., PEDREGOSA, Fabian, VAN MULBREGT, Paul, VIJAYKUMAR, Aditya, BARDELLI, Alessandro Pietro, ROTHBERG, Alex, HILBOLL, Andreas, KLOECKNER, Andreas, SCOPATZ, Anthony, LEE, Antony, ROKEM, Ariel, WOODS, C. Nathan, FULTON, Chad, MASSON, Charles, HÄGGSTRÖM, Christian, FITZGERALD, Clark, NICHOLSON, David A., HAGEN, David R., PASECHNIK, Dmitrii V., OLIVETTI, Emanuele, MARTIN, Eric, WIESER, Eric, SILVA, Fabrice, LENDERS, Felix, WILHELM, Florian, YOUNG, G., PRICE, Gavin A., INGOLD, Gert Ludwig, ALLEN, Gregory E., LEE, Gregory R., AUDREN, Hervé, PROBST, Irvin, DIETRICH, Jörg P., SILTERRA, Jacob, WEBBER, James T., SLAVIĆ, Janko, NOTHMAN, Joel, BUCHNER, Johannes, KULICK, Johannes, SCHÖNBERGER, Johannes L., DE MIRANDA CARDOSO, José Vinícius, REIMER, Joscha, HARRINGTON, Joseph, RODRÍGUEZ, Juan Luis Cano, NUNEZ-IGLESIAS, Juan, KUCZYNSKI, Justin, TRITZ, Kevin, THOMA, Martin, NEWVILLE, Matthew, KÜMMERER, Matthias, BOLINGBROKE, Maximilian, TARTRE, Michael, PAK, Mikhail, SMITH, Nathaniel J., NOWACZYK, Nikolai, SHEBANOV, Nikolay, PAVLYK, Oleksandr, BRODTKORB, Per A., LEE, Perry, MCGIBBON, Robert T., FELDBAUER, Roman, LEWIS, Sam, TYGIER, Sam, SIEVERT, Scott, VIGNA, Sebastiano, PETERSON, Stefan, MORE, Surhud, PUDLIK, Tadeusz, OSHIMA, Takuya, PINGEL, Thomas J., ROBITAILLE, Thomas P., SPURA, Thomas, JONES, Thouis R., CERA, Tim, LESLIE, Tim, ZITO, Tiziano, KRAUSS, Tom, UPADHYAY, Utkarsh, HALCHENKO, Yaroslav O. and VÁZQUEZ-BAEZA, Yoshiki. *SciPy 1.0: fundamental algorithms for scientific computing in Python*. *Nature Methods*. 2020. Vol. 17, no. 3, p. 261–272. <https://doi.org/10.1038/s41592-019-0686-2>.
28. *Rpi.GPIO Python Module*. Online. 0.7.1. Python 3. [Accessed 15 September 2022]. Available from:
29. HARRIS, Charles R., MILLMAN, K. Jarrod, VAN DER WALT, Stéfan J., GOMMERS, Ralf, VIRTANEN, Pauli, COURNAPEAU, David, WIESER, Eric, TAYLOR, Julian, BERG, Sebastian, SMITH, Nathaniel J., KERN, Robert, PICUS, Matti, HOYER, Stephan, VAN KERKWIJK, Marten H., BRETT, Matthew, HALDANE, Allan, DEL RÍO, Jaime Fernández, WIEBE, Mark, PETERSON, Pearu, GÉRARD-MARCHANT, Pierre, SHEPARD, Kevin, REDDY, Tyler, WECKESSER, Warren, ABBASI, Hameer, GOHLKE, Christoph and OLIPHANT, Travis E. *Array programming with NumPy*. *Nature*. 2020. Vol. 585, no. 7825, p. 357–362. <https://doi.org/10.1038/s41586-020-2649-2>.
30. MÜLLER, Swen and MASSARANI, Paulo. Transfer-Function Measurement with Sweeps. *Journal of the Audio Engineering Society*. 1 June 2001. Vol. 49.